A Jurassic acanthocephalan illuminates the origin of thorny-headed worms

Cihang Luo[1,2,3], Luke A. Parry[4], Brendon E. Boudinot[3], Shengyu Wang[1], Edmund A. Jarzembowski[1,5], Haichun Zhang[1], Bo Wang[1,*]

[1]State Key Laboratory of Palaeobiology and Stratigraphy, Nanjing Institute of Geology and Palaeontology, Chinese Academy of Sciences, Nanjing, China.

[2]University of Chinese Academy of Sciences, Beijing, China.

[3]Department of Terrestrial Zoology, Entomology II, Senckenberg Research Institute and Natural History Museum, Frankfurt am Main, Germany.

[4]Department of Earth Sciences, University of Oxford, Oxford, UK.

[5]Department of Earth Sciences, Natural History Museum, London, UK.

* Correspondence should be addressed to: B.W. (bowang@nigpas.ac.cn).

Summary

Acanthocephala (thorny-headed worms), characterised by the presence of an eversible proboscis with hooks, are a diverse endoparasitic group that infect a wide range of vertebrates and invertebrates[1]. While long regarded as a separate phylum, they have a number of putative sister taxa based on morphological features including Platyhelminthes (flatworms)[2], Priapulida (penis worms)[3] and Rotifera (wheel animals)[4]. Molecular phylogenies have instead recovered them within rotifers[5–10], suggesting acanthocephalans are derived from free-living worms with a jaw apparatus (Gnathifera). Their only fossil record is Late Cretaceous eggs[11], contributing limited palaeontological information to deciphering their early evolution. Here we describe the first acanthocephalan body fossil, *Juracanthocephalus daohugouensis* gen. et. sp. nov., from the Middle Jurassic Daohugou biota of China. *Juracanthocephalus*

exhibits unambiguous acanthocephalan characteristics, e.g. a hooked proboscis, a bursa, as well as a jaw apparatus with discrete elements that is typical of other gnathiferans. *Juracanthocephalus* shares features with Seisonidea (an epizoic member of Rotifera) and Acanthocephala, bridging the evolutionary gap between jawed rotifers and the obligate parasitic, jawless acanthocephalans. Our results reveal previously unrecognised ecological and morphological diversity in ancient Acanthocephala and highlight the significance of transitional fossils revealing the origins of this highly enigmatic group of living organisms.

Systematic palaeontology

Unranked clade Spiralia Scleip, 1929

Unranked clade Gnathifera Ahlrichs, 1995

Unranked clade Syndermata Zrzavý, 1998

Stem-group of Phylum Acanthocephala Koelreuter, 1771

Juracanthocephalus daohugouensis Luo, Parry & Wang, gen. et sp. nov.

Etymology. The generic name is derived from the combination of 'Jurassic' (referring the age of this fossil) and '*Acanthocephalus*' (the type genus of Acanthocephala). The species name is derived from 'Daohugou', which refers to the locality of the fossil. The gender is masculine.

Holotype. Specimen no. NIGP206848.

Locality and horizon. Ningcheng County, Chifeng City, Inner Mongolia, China; Daohugou Bed, Jiulongshan Formation (Middle Jurassic, around 165 million years old).

Diagnosis. Large acanthocephalan with jaw apparatus. Proboscis semi-oval, armed with approximately 26 spiral rows of 25–30 hooks in each row. Neck distinctly contracted. Trunk oval with nearly 40 lines of transverse combs.

Description and comparisons

Juracanthocephalus exhibits a remarkable preservation of soft tissues in tuffaceous mudstone. The specimen is nearly complete, retaining a well-defined body boundary with limited signs of decay (Fig. 1a, b and Extended Data Figs. 1–2). The majority of the specimen is laterally preserved, but the anterior one-third is twisted to dorsoventrally compressed. Our EDS analyses demonstrate that *Juracanthocephalus* is predominantly preserved as a thin carbonaceous compression, exhibiting elevated concentrations of carbon in the proboscis compared to the trunk. This observation may be attributed to differences in cuticle thickness and rigidity (Fig. 1b). A minor quantity of iron is present in the sediment but no association with the fossil is observed (Extended Data Fig. 1h). No calcium or phosphorus enrichments were detected, suggesting that *Juracanthocephalus* was not biomineralised or preserved via authigenic phosphatisation (Extended Data Fig. 1i). The posterior region of *Juracanthocephalus* is overlapped with fossil plants and an insect (dipteran) wing (Fig. 3e, f).

The body of *Juracanthocephalus* is fusiform, comprising a proboscis, neck and trunk (Fig. 1a–c and Extended Data Fig. 1). The total length of the specimen is 23.4 mm, with a maximum width of 8.4 mm. The proboscis is semi-oval in outline, 3.8 mm long and 3.6 mm wide. It is equipped with approximately 26 spiral rows of approximately 25–30 hooks in each row. The hooks are strongly sclerotised and gradually increase in size, the largest near the middle of the proboscis, then gradually

decrease in size, with a length ranging from 150–450 μm. The hooks are robust and exhibit only a slight curvature (Fig. 2a–d and Extended Data Fig. 2). Comparable hook-shaped sclerotised elements are also present in the introvert of scalidophorans (i.e. Priapulida, Kinorhyncha and Loricifera)[12,13] and extinct palaeoscolecids[14], as well as the tentacles of trypanorhynch cestodes[15]. However, scalidophorans and palaeoscolecids are exclusively marine and have never been found in freshwater where the fossil was deposited[16]. Additionally, their introverts are usually with less than 15 rows of hooks[17]. Palaeoscolecids became extinct after the Silurian, hundreds of millions of years earlier than the occurrence of *Juracanthocephalus*, which lacks the microplates that are commonly found in Palaeoscolecida[18]. Although marine trypanorhynchs have been discovered in terrestrial amber[19], they typically possess two or four armed tentacles[15], in contrast to the arrangement observed in *Juracanthocephalus*.

The potential mouth of *Juracanthocephalus* is situated in the ventral and subterminal part of the proboscis (Fig. 2a–d and Extended Data Fig. 2). The neck is short and strongly contracted. In lateral view, the trunk is oval and pseudo-segmented (Fig. 1 and Extended Data Fig. 1), with 32 prominent transverse combs one side which we identify as ventral based on comparison with extant taxa (e.g. Fig. 1e). The jaw apparatus is located in the anteriormost part of the trunk (Fig. 2e–l). The jaws are in converging paired rows, and their slight disarrayed and superposed appearance is likely a consequence of oblique burial. In general, the jaws become larger and more concave posteriad, exhibiting an increase in the number of teeth. Anteriorly, each jaw element is narrow at base and widens anteriorly, with numerous small teeth (Fig. 2e–i). The final two or three rows of jaws, however, maintain an almost constant width (Fig. 2e, f, j–l). While some acanthocephalans have hooks on the anterior trunk that

could be comparable to these features, in *Juracanthocephalus* they are oriented adaxially (i.e. directed toward the body axis), and anteriorly do not project beyond the body wall, which is clearly demarcated by the presence of carbon in elemental mapping (Fig. 1b). We therefore interpret these features as being internal, rather than external cuticular features.

A potential alimentary tract is preserved in the middle part of the proboscis (Fig. 2a–d and Extended Data Fig. 2f); the potential anus is located on the dorsal side, at about ¾ of the body length (Fig. 3e). No clear gut is visible within the trunk region. The jaw structures of *Juracanthocephalus*, however, are functional and homologous to gnathiferan jaws; their presence strongly implies that *Juracanthocephalus* had a gut. The bursa is quadrilateral, setaceous, 1.8 mm long and 0.8 mm wide (Fig. 3f).

The ventral surface of the trunk is ornamented by 38 lines of transverse, setaceous combs that are almost equidistant from one another, with 50–100 setae on each comb. The setae are 20–40 μm in length and are located anteriad (Fig. 3a–d). The transverse combs gradually increase in length and are longest at the middle part of the trunk, then gradually decrease in length, extending only to a small portion of the body. A comparable structure is observed in certain acanthocephalans such as *Serrasentis*[20] (Fig. 1e). While priapulids and palaeoscolecids are also annulated, the trunk rings typically traverse the entire body[12–14].

Phylogenetic affinities

To evaluate the precise phylogenetic position of *Juracanthocephalus*, we compiled a morphological matrix by assembling characters from published datasets of different vermiform phyla (the character list and complete reference list are provided in the Supplementary Note 1). Our parsimony and Bayesian phylogenetic analyses both

recover *Juracanthocephalus* as a crown-group gnathiferan (a clade characterised by its complex jaws made of chitin, comprising Gnathostomulida, Micrognathozoa and Syndermata)[21] and a stem-group acanthocephalan, sister to all extant acanthocephalans (Extended Data Figs. 3a, 4a and 5a). *Juracanthocephalus* can be regarded as a gnathiferan with confidence based on the presence of a jaw apparatus with discrete solid parts. It is further attributed to the Acanthocephala based on the hooked proboscis and the bursa; all these anatomical features are in accordance with the body plan of extant acanthocephalans[1,22]. *Juracanthocephalus* is distinct from all extant acanthocephalans in possessing a jaw apparatus, and potentially, also a mouth and an anus, features that are present in rotifers and other spiralians. Extant acanthocephalans lack these organs, having lost their digestive system, absorbing nutrients directly through the epidermis as a consequence of their endoparasitic lifestyle[22]. *Juracanthocephalus* therefore provides direct fossil evidence for a very early stage in the evolution of the acanthocephalan body plan, prior to the extensive reduction of the digestive system and jaw apparatus.

Analyses of morphological characters conflict regarding the affinities of acanthocephalans[2–4], but molecular phylogenetic analyses converge on placing them as a monophyletic group within Rotifera[5–10], forming the clade Syndermata (or Rotifera *sensu lato*), which encompasses both Acanthocephala and Rotifera *sensu stricto* (that is, Monogononta, Bdelloidea, and Seisonidea)[23]. However, the placement of Acanthocephala within Syndermata is still highly debated, with six competing hypotheses emerging from the results of molecular and morphological studies[24]. A sister group relationship between Bdelloidea and Monogononta (the Eurotatoria hypothesis) has previously been proposed based on morphological and ecological characteristics, with Acanthocephala identified as the most basal group within

Syndermata (Fig. 4a)[25], which is rejected by the molecular results[24]. A number of phylogenomic analyses support a close relationship with Seisonidea[8,10,24,26,27], forming the clade Pararotatoria, which is the sister group of Bdelloidea (Fig. 4b). Although Seisonidea and Acanthocephala were thought to have the similarities in epidermal ultrastructure and sperm morphology[4,28], the homology claims are dubious and details of sperm anatomy are conflicting[7]. Other phylogenomic studies have recovered Bdelloidea as the sister group to Acanthocephala (the Lemniscea hypothesis)[9,29] (Fig. 4c). Both proposed placements for Acanthocephala have previously lacked clear support from morphological evidence[27,30,31] and due to the lack of body fossils, the palaeontological record has shed no light on acanthocephalan origins.

Our discovery of *Juracanthocephalus* presents the first body fossil evidence of Acanthocephala. It exhibits a combination of anatomical features of Rotifera and Acanthocephala, bridging the evolutionary gap between these two groups. The inclusion/exclusion of *Juracanthocephalus* in our dataset can change the fundamental interrelationships between acanthocephalans and subclades of rotifers. Although Bayesian inference analyses fail to determine the precise position of Seisonidea among Syndermata (Extended Data Fig. 3), our strict consensus tree and 50% majority rule bootstrap consensus tree both recover Seisonidea as the sister group to *Juracanthocephalus* + all extant acanthocephalans, supported by the strongly depressed pharyngeal region (Fig. 4d and Extended Data Figs. 4–6). This result is consistent with the Pararotatoria hypothesis[8,10,24,26,27]. When *Juracanthocephalus* is excluded, the 50% majority rule bootstrap consensus tree support the Seisonidea as the sister group of all other Rotifera although with relatively low support value (Extended Data Fig. 5b), aligning with previous morphological analyses[7,32], while other analyses fail to determine the precise position of Seisonidea (Extended Data

Figs. 3b and 4b). Consequently, our study indicates that *Juracanthocephalus* is a key transitional taxon that reconciles conflict between morphology and the majority of phylogenomic analyses[8,10,24,26,27], offering insights into the early evolution of morphological features and lifestyles of Acanthocephala. This result further emphasises the impact of *Juracanthocephalus* on the phylogeny of Syndermata, underscoring the importance of pivotal fossils in resolving difficult nodes in animal phylogeny[33].

Evolution of the Acanthocephala

The majority of endoparasitic worms are poorly represented in the fossil record as they are small and soft bodied. Consequently, the fossil record of these groups is normally limited to relatively recalcitrant features, such as attachment hooks, eggs and cocoons[34]. The fossil record therefore usually sheds little light on the origins of parasites, which are typically highly morphologically modified with respect to their close relatives. Therefore, the sequence of character state changes leading to a parasitic lifestyle and the placement in these groups on the tree of life are often highly controversial[34]. For Acanthocephala, one hypothesis proposed that they emerged during the Cambrian Period, alongside a diverse and abundant marine arthropod fauna, switching from the free-living/epizoic lifestyle of the syndermatan ancestors to a parasitic lifestyle in aquatic arthropods[22]. However, this scenario lacks any direct fossil evidence and the only previous definite fossils of Acanthocephala are four Late Cretaceous eggs discovered in the coprolites of crocodyliformes (approximately 72 million years old)[11].

As a stem-group acanthocephalan, *Juracanthocephalus* provides a crucial reference point for investigating the origins of their evolutionary novelties and body

plan. The hooked proboscis is the most notable feature of the acanthocephalans, representing a specialised organ for endoparasitic habits. The rings of recurved hooks are arranged in horizontal or spiral rows, and acanthocephalans attach themselves to the gut of their hosts using their armed proboscis[22]. Therefore, this feature indicates that *Juracanthocephalus* was an endoparasite. In contrast to extant Acanthocephala, *Juracanthocephalus* was probably unable to absorb nutrients solely through the epidermis due to the presence of the jaw apparatus and a possible alimentary system.

The most intriguing feature of *Juracanthocephalus* is its jaw apparatus composed of clustered, tooth-like units that can be seen in the jaws of Gnathostomulida and Micrognathozoa[32]. It is clearly an internal structure because unlike the external hooks, spines or sclerites of the introvert of priapulids[12] or palaeoscolecid worms[14], or trunk hooks of certain acanthocephalans[35], none of the jaw elements of *Juracanthocephalus* project beyond the body margin. Gnathiferans are characterised by having pharyngeal jaws that are bilaterally symmetrical in dorsal view, but the majority of our specimen is laterally preserved. However, the anterior one-third including the proboscis and the jaw area is twisted to dorsoventrally compressed based on the evidence that transverse combs are increasingly intersecting anteriad. Meanwhile, the front part of the dorsal side of the fossil is partly destroyed (Fig. 1a–c), which may cause certain loss of jaw elements. Consequently, taphonomic deformation has resulted in the jaw apparatus appearing to be not strictly bilaterally symmetrical. In almost all gnathiferans, the jaws are situated within or before the pharyngeal region[36], but in *Juracanthocephalus,* the jaws are situated behind the neck region. Furthermore, the presence of repeated similar elements is unlike that of typical gnathiferan jaws, where the elements are in bilateral pairs or single unpaired bilaterally symmetrical elements (e.g. the basal plate of Gnathostomulida), which is the likely ancestral condition shared with

chaetognaths[36,37]. This arrangement in a stem group acanthocephalan therefore represents an unexpected anatomical (and presumably functional) modification of the jaw apparatus, prior to its total loss in the crown group.

Juracanthocephalus is comparatively large, with a length exceeding 20 mm. This is consistent with extant acanthocephalans, which typically range from less than 1 millimetre to a few centimetres, exceptionally reaching 20 cm or more in few species[22]. The size of *Juracanthocephalus* suggests that it already utilised vertebrates as a host, being too large for the known Daohugou arthropods to act as its final hosts[16]. In the Daohugou Lagerstätte, more than 30 vertebrate taxa have been described including salamanders, lizards, pterosaurs, dinosaurs and mammals[38]. Several are sufficiently large to serve as a host of *Juracanthocephalus*. While the majority of gnathiferans are submillimetric benthic worms[39], members of the Seisonidea can reach a length of 2.5 mm[40], although this is still a considerably smaller size than that of *Juracanthocephalus*. Therefore, the relatively large size of *Juracanthocephalus* provides further evidence to support the adaptation to a vertebrate endoparasitic lifestyle[22].

Nevertheless, an endoparasitic lifestyle would typically represent a challenge to preservation as a completely soft bodied fossil. Preservation of an endoparasitic acanthocephalan from the extrinsic environment is a possibility, given that this has been documented in extant taxa[41]. Thus, *Juracanthocephalus* could have met an unsuitable host which expelled the parasite[42]. Alternatively, it may have left the host before or after oviposition, as is the case with some extant acanthocephalan species[43]. During the Middle Jurassic, the Daohugou area was characterised by the presence of shallow, short-lived lakes or ponds. The active volcanism that occurred at the time resulted in the simultaneous death of animals occupying a range of ecological niches,

which were then rapidly buried[16]. It is therefore plausible that *Juracanthocephalus* met its end in a volcanic eruption shortly after leaving its host, resulting in its rapid entombment in ash.

Body fossils of gnathiferans are incredibly rare and *Juracanthocephalus* provides an important record of crown-group Gnathifera prior to the Cretaceous. The oldest fossils with gnathiferan-like jaws are from the Cambrian[36,44], but most are regarded as chaetognaths (the gnathiferan sister group) rather than gnathiferans *sensu stricto*[21,37] (although see ref. 36 regarding potential rotifer affinities of the Cambrian fossil *Inquicus*). Only a limited number of rotifer fossils have been discovered, i.e. a possible rotifer lorica from a Jurassic hot spring chert in Argentina[45], a monogonont from the Eocene of South Australia[46] and bdelloids from Miocene Dominican amber[47,48]. The discovery of a Jurassic stem-acanthocephalan provides evidence that, although there is still no confirmed evidence to prove Syndermata originated in the Palaeozoic as previously proposed[3,22], they diverged at least before the Middle Jurassic.

The discovery of a terrestrial stem-group acanthocephalan provides new insights into the evolution of acanthocephalan endoparasitism. While almost all rotifers are free-living, Seisonidea are epizoic on marine crustaceans[24]. However, Archiacanthocephala, the sister group of all other extant acanthocephalans, are completely terrestrial and utilise insects and myriapods as intermediate hosts, with predatory birds and mammals acting as final hosts[22]. The discovery of a stem acanthocephalan from the Daohugou biota therefore indicates that Acanthocephala may have terrestrial rather than marine origins, with multiple subsequent colonization events of marine hosts[49].

The conserved jaw structure in *Juracanthocephalus* represents a plesiomorphy

that was inherited from a more gnathiferan-like common ancestor, prior to their loss in crown-group Acanothocephala. The unique character combination exhibited by *Juracanthocephalus* suggests that a bursa and hooked proboscis for attachment to a host evolved prior to the reduction and loss of the digestive system, shedding light on the transition from a free-living worm to a highly specialised endoparasite. The unique combination of anatomical features in *Juracanthocephalus* provides new palaeontological evidence that reconciles morphological and molecular analyses into the systematic position of Acanthocephala among Gnathifera. While molecular phylogenetics offers a robust approach for reconstructing the relationships across the entire tree of life, challenging numerous enigmas based on morphological characters alone[50], *Juracanthocephalus* emphasises the role that transitional fossils play in revealing how and when radical morphological changes in animal body plans took place.

Online content

Any methods, additional references, Nature Portfolio reporting summaries, source data, extended data, supplementary information, acknowledgements, peer review information; details of author contributions and competing interests; and statements of data and code availability are available at https://doi.org/

1 Kennedy, C. R. *Ecology of the Acanthocephala* (Cambridge University Press, 2006).

2 Van Cleave, H. J. Relationships of the Acanthocephala. *Am. Nat.* **75**, 31–47 (1941).

3 Conway Morris, S. & Crompton, D. W. T. The origins and evolution of the

Acanthocephala. *Biol. Rev.* **57**, 85–115 (1982).

4 Ahlrichs, W. H. Epidermal ultrastructure of *Seison nebaliae* and *Seison annulatus*, and a comparison of epidermal structures within the Gnathifera. *Zoomorphology* **117**, 41–48 (1997).

5 Garey, J. R., Near, T. J., Nonnemacher, M. R. & Nadler, S. A. Molecular evidence for Acanthocephala as a subtaxon of Rotifera. *J. Mol. Evol.* **43**, 287–292 (1996).

6 Herlyn, H., Piskurek, O., Schmitz, J., Ehlers, U. & Zischler, H. The syndermatan phylogeny and the evolution of acanthocephalan endoparasitism as inferred from 18S rDNA sequences. *Mol. Phylogenet. Evol.* **26**, 155–164 (2003).

7 Sørensen, M. V. & Giribet, G. A modern approach to rotiferan phylogeny: Combining morphological and molecular data. *Mol. Phylogenet. Evol.* **40**, 585–608 (2006).

8 Wey-Fabrizius, A. R. *et al.* Transcriptome data reveal syndermatan relationships and suggest the evolution of endoparasitism in Acanthocephala via an epizoic stage. *PLOS ONE* **9**, e88618 (2014).

9 Laumer, C. E. *et al.* Spiralian phylogeny informs the evolution of microscopic lineages. *Curr. Biol.* **25**, 2000–2006 (2015).

10 Sielaff, M. *et al.* Phylogeny of Syndermata (syn. Rotifera): Mitochondrial gene order verifies epizoic Seisonidea as sister to endoparasitic Acanthocephala within monophyletic Hemirotifera. *Mol. Phylogenet. Evol.* **96**, 79–92 (2016).

11 Cardia, D. F. F., Bertini, R. J., Camossi, L. G. & Letizio, L. A. First record of Acanthocephala parasites eggs in coprolites preliminary assigned to

Crocodyliformes from the Adamantina Formation (Bauru Group, Upper Cretaceous), São Paulo, Brazil. *An. Acad. Bras. Ciênc.* **91**, e20170848 (2019).

12 Smith, M. R., Harvey, T. H. P. & Butterfield, N. J. The macro- and microfossil record of the Cambrian priapulid *Ottoia*. *Palaeontology* **58**, 705–721 (2015).

13 Giribet, G. & Edgecombe, G. D. Current understanding of Ecdysozoa and its internal phylogenetic relationships. *Integr. Comp. Biol.* **57**, 455–466 (2017).

14 Smith, M. R. A palaeoscolecid worm from the Burgess Shale. *Palaeontology* **58**, 973–979 (2015).

15 Palm, H. W. *The Trypanorhyncha Diesing, 1863* (PKSPL-IPB Press, 2004).

16 Wang, S. *et al.* High-resolution taphonomic and palaeoecological analyses of the Jurassic Yanliao Biota of the Daohugou area, northeastern China. *Palaeogeogr. Palaeoclim. Palaeoecol.* **530**, 200–216 (2019).

17 Yang, J., Smith, M. R., Zhang, X.-g. & Yang, X.-y. Introvert and pharynx of *Mafangscolex*, a Cambrian palaeoscolecid. *Geol. Mag.* **157**, 2044–2050 (2020).

18 Howard, R. J., Parry, L. A., Clatworthy, I., D'Souza, L. & Edgecombe, G. D. Palaeoscolecids from the Ludlow Series of Leintwardine, Herefordshire (UK): the latest occurrence of palaeoscolecids in the fossil record. *Pap. Palaeontol.* **10**, e1558 (2024).

19 Luo, C. *et al.* Exceptional preservation of a marine tapeworm tentacle in Cretaceous amber. *Geology* **52**, 497–501 (2024).

20 Fonseca, M. C. G. d. *et al.* Acanthocephalan parasites of the flounder species *Paralichthys isosceles*, *Paralichthys patagonicus* and *Xystreurys rasile* from Brazil. *Rev. Bras. Parasitol. V.* **28**, 346–359 (2019).

21 Bekkouche, N. & Gąsiorowski, L. Careful amendment of morphological data

sets improves phylogenetic frameworks: re-evaluating placement of the fossil *Amiskwia sagittiformis*. *J. Syst. Palaeontol.* **20**, 1–14 (2022).

22 Herlyn, H. in *The Evolution and Fossil Record of Parasitism: Identification and Macroevolution of Parasites* (eds De Baets, K. & Huntley, J. W.) 273–313 (Springer International Publishing, 2021).

23 Ahlrichs, W. H. *Zur Ultrastruktur und Phylogenie von* Seison nebaliae *Grube, 1859 und* Seison annulatus *Claus, 1876. Hypothesen zu phylogenetischen Verwandtschaftsverhältnissen innerhalb der Bilateria* (Georg-August-University, 1995).

24 Vasilikopoulos, A. *et al.* Whole-genome analyses converge to support the Hemirotifera hypothesis within Syndermata (Gnathifera). *Hydrobiologia* **851**, 2795–2826 (2024).

25 Melone, G., Ricci, C., Segers, H. & Wallace, R. L. Phylogenetic relationships of phylum Rotifera with emphasis on the families of Bdelloidea. *Hydrobiologia* **387**, 101–107 (1998).

26 Mauer, K. M. *et al.* Genomics and transcriptomics of epizoic Seisonidea (Rotifera, syn. Syndermata) reveal strain formation and gradual gene loss with growing ties to the host. *BMC Genomics* **22**, 604 (2021).

27 Hagemann, L., Mauer, K. M., Hankeln, T., Schmidt, H. & Herlyn, H. Nuclear genome annotation of wheel animals and thorny-headed worms: inferences about the last common ancestor of Syndermata (Rotifera *s.l.*). *Hydrobiologia* **851**, 2827–2844 (2023).

28 Ferraguti, M. & Melone, G. Spermiogenesis in *Seison nebaliae* (Rotifera, Seisonidea): further evidence of a rotifer-acanthocephalan relationship. *Tissue Cell* **31**, 428–440 (1999).

29 Struck, T. H. *et al.* Platyzoan paraphyly based on phylogenomic data supports a noncoelomate ancestry of Spiralia. *Mol. Biol. Evol.* **31**, 1833–1849 (2014).

30 Clément, P. The phylogeny of rotifers: molecular, ultrastructural and behavioural data. *Hydrobiologia* **255**, 527–544 (1993).

31 Ricci, C. Are lemnisci and proboscis present in the Bdelloidea? *Hydrobiologia* **387**, 93–96 (1998).

32 Sørensen, M. V. On the evolution and morphology of the rotiferan trophi, with a cladistic analysis of Rotifera. *J. Zool. Syst. Evol. Res.* **40**, 129–154 (2002).

33 Koch, N. M. & Parry, L. A. Death is on our side: paleontological data drastically modify phylogenetic hypotheses. *Syst. Biol.* **69**, 1052–1067 (2020).

34 De Baets, K., Dentzien-Dias, P., Harrison, G. W. M., Littlewood, D. T. J. & Parry, L. A. in *The Evolution and Fossil Record of Parasitism: Identification and Macroevolution of Parasites* (eds De Baets, K. & Huntley, J. W.) 231–271 (Springer International Publishing, 2021).

35 Verweyen, L., Klimpel, S. & Palm, H. W. Molecular phylogeny of the Acanthocephala (class Palaeacanthocephala) with a paraphyletic assemblage of the orders Polymorphida and Echinorhynchida. *PLOS ONE* **6**, e28285 (2011).

36 Vinther, J. & Parry, L. A. Bilateral jaw elements in *Amiskwia sagittiformis* bridge the morphological gap between gnathiferans and chaetognaths. *Curr. Biol.* **29**, 881–888 (2019).

37 Park, T.-Y. S. *et al.* A giant stem-group chaetognath. *Sci. Adv.* **10**, eadi6678 (2024).

38 Sullivan, C. *et al.* The vertebrates of the Jurassic Daohugou Biota of northeastern China. *J. Vertebr. Paleontol.* **34**, 243–280 (2014).

401 39 Hejnol, A. in *Evolutionary Developmental Biology of Invertebrates 2:*
402 *Lophotrochozoa (Spiralia)* (ed Wanninger, A.) 1–12 (Springer Vienna, 2015).
403 40 Ricci, C., Melone, G. & Sotgia, C. Old and new data on Seisonidea (Rotifera).
404 *Hydrobiologia* **255**, 495–511 (1993).
405 41 Haustein, T., Lawes, M., Harris, E. & Chiodini, P. L. An eye-catching
406 acanthocephalan. *Clin. Microbiol. Infec.* **16**, 787–788 (2010).
407 42 Nickol, B. B. in *Fish Diseases and Disorders, Volume 1: Protozoan and*
408 *Metazoan Infections* (ed Woo, P. T. K.) 444–465 (CAB International, 2006).
409 43 Al-Jahdali, M. O., Hassanine, R. M. E.-S. & Touliabah, H. E.-S. The life cycle
410 of *Sclerocollum saudii* Al-Jahdali, 2010 (Acanthocephala:
411 Palaeacanthocephala: Rhadinorhynchidae) in amphipod and fish hosts from
412 the Red Sea. *J. Helminthol.* **89**, 277–287 (2015).
413 44 Cong, P. *et al.* Host-specific infestation in early Cambrian worms. *Nat. Ecol.*
414 *Evol.* **1**, 1465–1469 (2017).
415 45 Massini, J. G., Escapa, I. H., Guido, D. M. & Channing, A. First glimpse of
416 the silicified hot spring biota from a new Jurassic chert deposit in the Deseado
417 Massif, Patagonia, Argentina. *Ameghiniana* **53**, 205–230 (2016).
418 46 Southcott, R. V. & Lange, R. T. Acarine and other microfossils from the
419 Maslin Eocene, South Australia. *Rec. S. Aust. Mus.* **16**, 1–21 (1971).
420 47 Poinar, G. O. & Ricci, C. Bdelloid rotifers in Dominican amber: Evidence for
421 parthenogenetic continuity. *Experientia* **48**, 408–410 (1992).
422 48 Waggoner, B. M. & Poinar, G. O. Fossil habrotrochid rotifers in Dominican
423 amber. *Experientia* **49**, 354–357 (1993).
424 49 Near, T. J., Garey, J. R. & Nadler, S. A. Phylogenetic relationships of the
425 Acanthocephala inferred from 18S ribosomal DNA sequences. *Mol.*

Phylogenet. Evol. **10**, 287–298 (1998).

50 Kapli, P., Yang, Z. & Telford, M. J. Phylogenetic tree building in the genomic age. *Nat. Rev. Genet.* **21**, 428–444 (2020).

Figure legends

Fig. 1 | Gross morphology of holotype of *J. daohugouensis* gen. et sp. nov., NIGP206848, and the comparsion with extant Acanthocephala. a, Overall view (dry). **b**, Elemental maps of carbon of **a** from energy-dispersive X-ray spectroscopy, showing proboscis, jaw apparatus and transverse combs with positive signal. **c**, Line drawing of **a**. **d**, Artistic reconstruction by D. Yang. **e**, The lateral view of an extant acanthocephalan juvenile male of *Serrasentis sagittifer* (Palaeacanthocephala: Rhadinorhynchidae)[20]; courtesy of Marcelo Knoff, Instituto Oswaldo Cruz, Brasil. au, anus; bu, bursa; ja, jaw apparatus; mo, mouth; tc, transverse combs; pb, proboscis. Scale bars, 2.0 mm (**a**–**d**), 0.5 mm (**e**).

Fig. 2 | Proboscis and jaw apparatus of *J. daohugouensis* gen. et sp. nov., NIGP206848. a, Overall view showing the regions of interest. **b**–**d**, Proboscis. **b**, Microscopic image (in alcohol), note the alimentary tract. **c**, Backscatter scanning electron image under a scanning electronic microscope, white arrows mark hooks. **d**, Elemental map of C (green colour), Si (purple colour), and K (yellow colour) concentrations from energy-dispersive X-ray spectroscopy. **e–l**, Jaw apparatus. **e**, Overall view (in alcohol). **f**, Line drawing of **e**. **g**, Superposed jaws in the anterior part. **h**, Two distinct jaws with teeth and setae. **i**, Scanning electron microscope (SEM) image of the apical part of an anterior jaw. **j**, Two enlarged posterior jaws. **k**, Another two enlarged posterior jaws from the other side. **l**, SEM image of the apical part of a posterior jaw. at, alimentary tract; mo, mouth. All analyses were performed three times. Scale bars, 5.0 mm (**a**), 1.0 mm (**b**–**f**), 0.1 mm (**g**, **h**, **j**, **k**), 50 μm (**i**, **l**).

Fig. 3 | Posterior area of *J. daohugouensis* gen. et sp. nov., NIGP206848. a, Overall view showing the regions of interest. **b**, Several lines of transverse combs (in alcohol). **c**, Line drawing of **b**. **d**, One transverse comb composed of numerous setae

(in alcohol), white arrows mark setae. **e**, The anal area (in alcohol), note a wing of a dipteran that overlaps *J. daohugouensis*. **f**, Bursa (in alcohol), note the black fragment is plant debris. au, anus; bu, bursa; dw, dipteran wing; tc, transverse combs; tr, trunk; pd, plant debris. All analyses were performed three times. Scale bars, 5.0 mm (**a**), 1.0 mm (**e**), 0.5 mm (**b**, **c**, **f**), 0.2 mm (**d**).

Fig. 4 | Represetiative hypotheses concerning the phylogenetic relationships of Syndermata and the phylogenetic position of *J. daohugouensis*. a, Pararotatoria hypothesis (Seisonidea and Acanthocephala are sister groups) and Hemirotifera hypothesis (Monogononta is the sister group of a clade Acanthocephala + Bdelloidea + Seisonidea). **b**, Seisonidea-sister hypothesis (Seisonidea is the sister group of a clade Acanthocephala + Bdelloidea + Monogononta) and Lemniscea hypothesis (Acanthocephala and Bdelloidea are sister groups). **c**, Acanthocephala-sister hypothesis (Acanthocephala is the sister group of Rotifera *sensu stricto*) and Eurotatoria hypothesis (Bdelloidea and Monogononta are sister groups). **d**, Simplified cladogram of Gnathifera showing *Juracanthocephalus* in red box. The topology is derived from the strict consensus tree based on a matrix of 68 taxa and 247 characters (Extended Data Fig. 6 and Supplementary Data 2); the non-gnathiferans were omitted for clarity; the precise systematic position of Gnathostomulida has not been recovered in the strict consensus tree, but it is widely considered as the sister group of other gnathiferans. The rectangles denote important apomorphies optimised computationally, and the apomorphic losses of Acanthocephala are also added (a comprehensive list of apomorphies is provided in Extended Data Fig. 6); yellow rectangles represent characters associated with jaw apparatus, green rectangles represent characters associated with alimentary tract (including mouth and anus), red rectangles represent characters associated with body shape, and grey rectangles

represent characters associated with other body structures. The characters that can be observed in *J. daohugouensis* are in red colour, otherwise in black. Cross indicates extinct taxa.

Methods

Observation

The specimen described herein was observed under a Zeiss Stemi 508 microscope, equipped with polarizing filters, and photographed both in a dry state and in a wet state under natural and cross-polarised lighting conditions. The photographs were taken with a Zeiss Stereo Discovery V16 microscope system at the Nanjing Institute of Geology and Palaeontology, Chinese Academy of Sciences (NIGPAS). Photomicrographic composites of 5–30 individual focal planes were digitally stacked using the Helicon Focus 6.7.1 software (https://www.heliconsoft.com/heliconsoft-products/helicon-focus/) to enhance the illustration of three-dimensional (3-D) structures. Figures were produced using Adobe Photoshop 25.11.0 and CorelDRAW 2022 graphic software.

Material

The specimen NIGP206848 studied here comes from the Middle Jurassic Jiulongshan Formation of Daohugou (41°18′N, 119°13′E) in Ningcheng County, Chifeng City, Inner Mongolia, China. The Daohugou fossil-bearing strata consist of mainly grayish-white tuff, tuffaceous sandstone, siltstone, and shale, with a tuffaceous conglomerate at the base and a thick rhyolitic breccia and andesite at the top. The age of the fossil-bearing strata is considered to be late Middle Jurassic. The fossils are commonly preserved as carbonaceous compressions on the surface of grey tuffaceous siltstones[16]. NIGP206848 is permanently deposited in NIGPAS.

Scanning electron microscopy and energy-dispersive X-ray spectroscopy analyses

The SEM (scanning electron microscope) and EDS (X-ray energy dispersive spectrum) analyses were conducted at NIGPAS. The SEM images were obtained

using a Tescan Maia 3 GMU scanning electron microscope in high vacuum mode at an accelerating voltage of 10 kV and a working distance of 9.8 mm. The elemental analyses were undertaken with a scanning electron microscope Zeiss Crossbeam 550 in high vacuum mode at an accelerating voltage of 15 kV with a working distance of 8–9 mm. To obtain a higher resolution of element C, the elemental analyses were conducted at an accelerating voltage of 5 kV. Individual frames were captured an average of 385 full spectral X-ray images, with a resolution of 1024*768 pixels and 80 s per image—a dwell time of 100 µs per pixel. The total run time was 8–9 hours. All images were montaged with a 10% overlap.

Phylogenetic analysis

See Supplementary Note 1 for further details regarding the phylogenetic dataset, characters, and character scores. Our matrix includes 68 taxa and 247 morphological characters, which were analysed using parsimony and Bayesian approaches. Two separate analyses were conducted for each approach, the first of which included all taxa, while the second excluded *Juracanthocephalus*. The outgroup was specified to include Tardigrada, Onychophora, Arthropoda, Nematoda, Nematomorpha, Kinorhyncha, *Priapulus caudatus* (Priapulida), and *Nanaloricus mysticus* (Loricifera). Phylogenetic analyses were performed in MrBayes 3.2.7a[51] (Supplementary Data 1). Analyses used the Mk-inf + gamma model (correction for scoring rate variation among characters modeled as a gamma distribution)[52]. Two million generations were requested, and analyses were terminated automatically when the average standard deviation (SD) of split frequencies was below 0.01. Convergence was evaluated using effective sample size (ESS) (>200) and potential scale reduction factor (PRSF) (~1.0) values for each parameter. The results of phylogenetic analyses are presented in Extended Data Fig. 3.

The parsimony analyses (Supplementary Data 2) were conducted using the phylogenetic analysis software PAUP* (v. 4.0a169)[53] with the heuristic search strategies started from 1,000 random addition sequences. The number of trees held at each step was automatically increased, and the tree bisection and reconnection (TBR) algorithm was employed in PAUP. All characters were non-additive and unordered. The analyses including *Juracanthocephalus* yielded a total of 593 most parsimonious trees of 410 scores each (consistency index = 0.566; retention index = 0.834), while the analyses excluding *Juracanthocephalus* produced 659 most parsimonious trees of 409 scores each (consistency index = 0.567; retention index = 0.833). The strict consensus trees, calculated from the most parsimonious trees, are presented in Extended Data Fig. 4. A non-parametric bootstrap search based on 1,000 replicates was conducted using a heuristic search algorithm in PAUP, with starting trees built using stepwise addition and branch swapping undertaken using TBR. The results of this bootstrap analysis are summarized as a 50% majority rule consensus tree (Extended Data Fig. 5).

The apomorphies were calculated in TNT (v.1.6)[54] using a parsimony ratchet and TBR branch swapping with 10,000 replicates, holding 100 trees from each iteration (Supplementary Data 3). This resulted in 4,390 equally parsimonious trees with a length of 410 scores. Then, the apomorphies were optimised computationally using the ‘mapping common synapomorphies’ function in TNT after estimating the consensus trees. The apomorphies of Gnathifera are presented in Extended Data Fig. 6.

Reporting summary

Further information on research design is available in the Nature Portfolio Reporting

Summary linked to this article.

Data availability

All data analysed in this paper, including the phylogenetic datasets, are available as part of the Article, Extended Data Figs. 1–6 or Supplementary Information. The nomenclature of *J. daohugouensis* gen. et sp. nov. has been registered at ZooBank (LSID: urn:lsid:zoobank.org:act:4F294930-AE20-45E4-A9E2-8FC96919B56B).

Code availability

The phylogenetic datasets and the commands necessary for executing the MrBayes, PAUP and TNT analyses are included as NEXUS and TNT formatted files in the Supplementary Data 1–3.

51 Huelsenbeck, J. P. & Ronquist, F. MRBAYES: Bayesian inference of phylogenetic trees. *Bioinformatics* **17**, 754–755 (2001).

52 Lewis, P. O. A likelihood approach to estimating phylogeny from discrete morphological character data. *Syst. Biol.* **50**, 913–925 (2001).

53 Swofford, D. L. PAUP*. Phylogenetic Analysis Using Parsimony (* and Other Methods) Version 4. (Sinauer Associates, 2003).

54 Goloboff, P. A. & Morales, M. E. TNT version 1.6, with a graphical interface for MacOS and Linux, including new routines in parallel. *Cladistics* **39**, 144–153 (2023).

Acknowledgments We are grateful to H. Herlyn, H. Zhang, M.V. Sørensen, A. Rasnitsyn, J. Zhang, and D. Zheng for helpful discussions and comments, Y. Fang for the energy-dispersive X-ray spectroscopy analyses, and D. Yang for artistic reconstruction. We also thank Marcelo Knoff for providing the image of *Serrasentis sagittifer*. This study was supported by the National Natural Science Foundation of China (42125201, 42293280).

Author contributions B.W. designed the project; C.L., L.A.P. and B.E.B. carried out the phylogenetic analysis; S.W. conducted the scanning electron microscopy and energy-dispersive X-ray spectroscopy analyses; H.Z. and B.W. collected the specimen; C.L., L.A.P. and B.W. wrote the original draft with review and editing from B.E.B., S.W., E.A.J. and H.Z. All authors carried out the morphological analysis, discussed the results and approved the final manuscript.

Competing interests The authors declare no competing interests.

Additional information

Supplementary information

The online version contains supplementary material available at https://doi.org/

Correspondence and requests for materials should be addressed to Bo Wang.

Peer review information *Nature* thanks Tae-Yoon S. Park and the other, anonymous, reviewer(s) for their contribution to the peer review of this work.

Reprints and permissions information is available at http://www.nature.com/reprints.

Extended Data

Extended Data Figure Captions

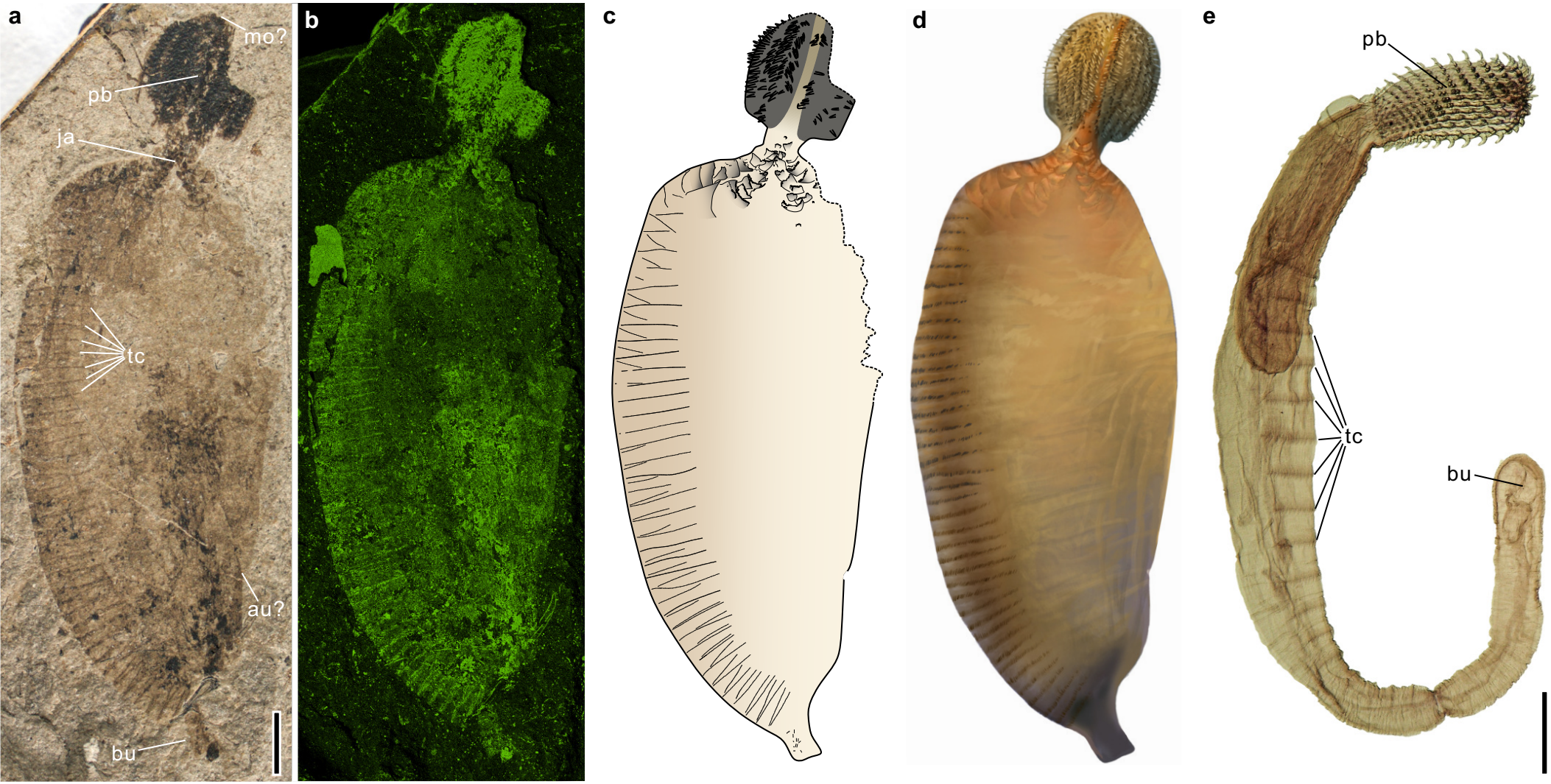
Extended Data Fig. 1 | Elemental analysis of holotype of *J. daohugouensis* gen. et sp. nov., NIGP206848. a, Photograph in alcohol. **b**, Backscatter scanning electron (BSE) image under a scanning electronic microscope. **c**–**h**, Elemental maps of **b** from energy-dispersive X-ray spectroscopy. **c**, Overlay image of element C (green colour), O (red colour), Al (blue colour), Si (purple colour), and K (yellow colour) concentrations. **d**, O map. **e**, Al map. **f**, Si map. **g**, K map. **h**, Fe map. **i**, EDS spectrum of the complete montage. Scale bar, 2.0 mm.

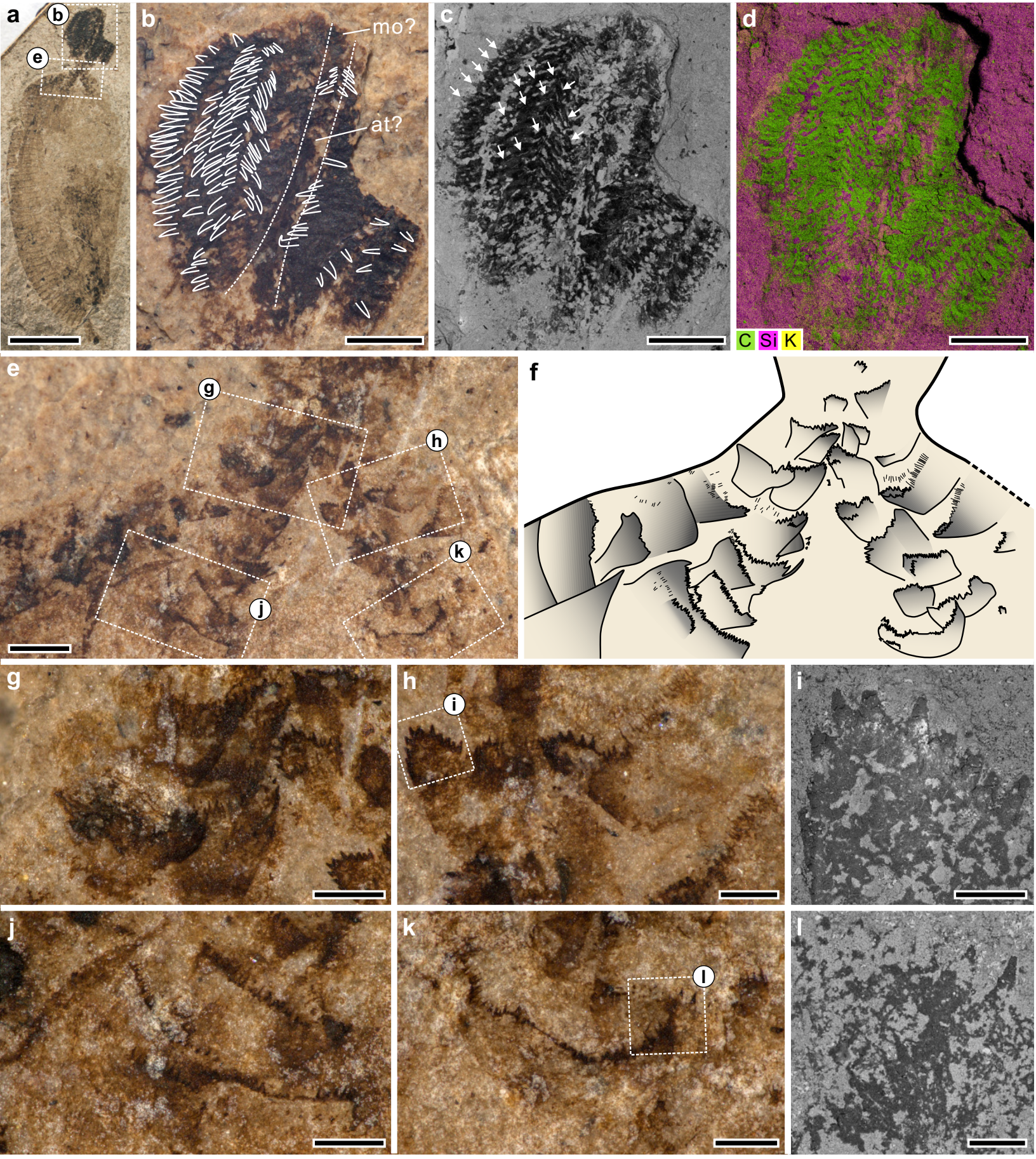
Extended Data Fig. 2 | Proboscis of holotype of *J. daohugouensis* gen. et sp. nov., NIGP206848. a–**d**, Elemental maps from energy-dispersive X-ray spectroscopy. **a**, C map. **b**, O map. **c**, Si map. **d**, K map. **e**, Higher magnification of proboscis (dry), white arrows mark hooks. **f**, Higher magnification of mouth opening area (in alcohol). at, alimentary tract. All analyses were performed three times. Scale bars, 0.5 mm (**a**–**d**), 0.2 mm (**e**, **f**).

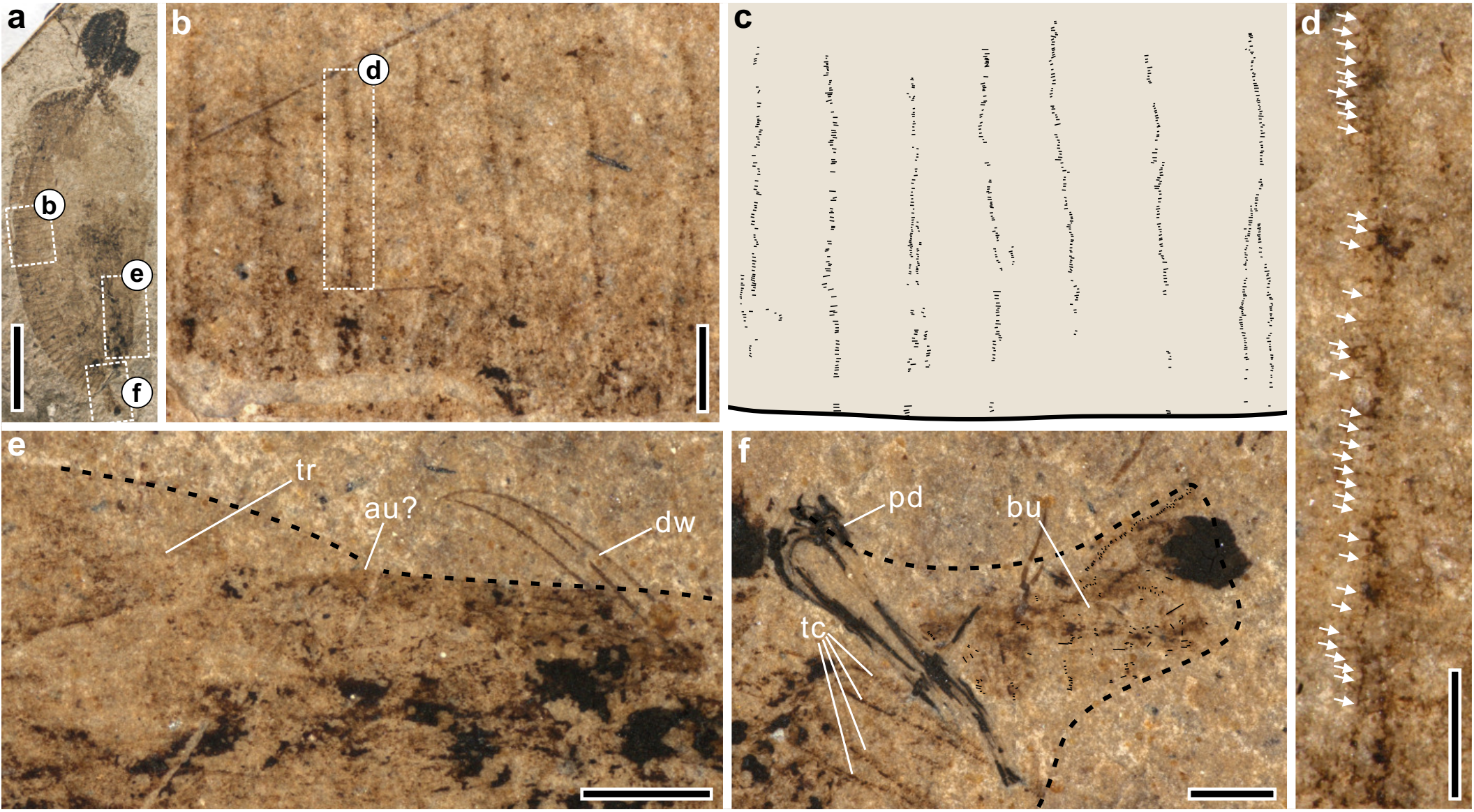
Extended Data Fig. 3 | Topology from Bayesian inference phylogenetic analysis. **a**, Majority-rule consensus tree including *J. daohugouensis* from Bayesian inference analysis (Methods). **b**, Majority-rule consensus tree excluding *J. daohugouensis* from Bayesian inference analysis (Methods). Node labels show posterior probability values.

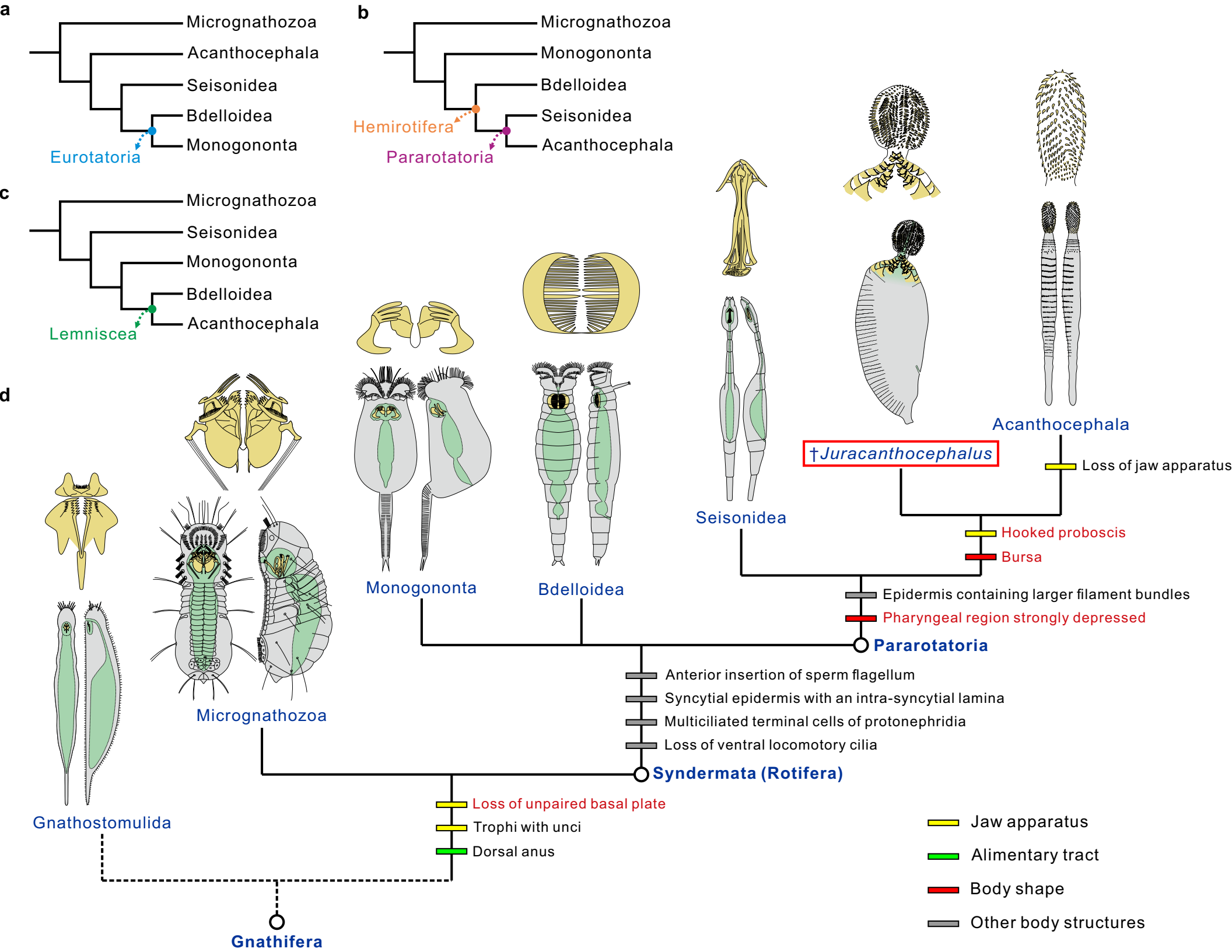
Extended Data Fig. 4 | Phylogenetic tree from strict consensus tree of parsimony analysis. a, Strict consensus tree including *J. daohugouensis* of 593 most parsimonious trees (410 scores each) from PAUP parsimony analysis (Methods), CI = 0.566, RI = 0.834. **b**, Strict consensus tree excluding *J. daohugouensis* of 659 most parsimonious trees (409 scores each) from PAUP parsimony analysis (Methods), CI =

626 0.567, RI = 0.833. The strict consensus tree fails to resolve the relationship between
627 Seisonidea, Rotifera and Acanthophala when *Juracanthocephalus* is excluded.
628 **Extended Data Fig. 5 | Phylogenetic tree from 50% majority rule bootstrap**
629 **consensus tree of parsimony analysis. a**, 50% majority rule bootstrap consensus tree
630 including *J. daohugouensis* from PAUP parsimony analysis (Methods). **b**, 50%
631 majority rule bootstrap consensus tree excluding *J. daohugouensis* from PAUP
632 parsimony analysis (Methods). Node labels indicate bootstrap support.
633 **Extended Data Fig. 6 | Full list of apomorphies of Gnathifera.** Apomorphies are
634 optimized computationally unless followed by an asterisk, which denotes an
635 apomorphy suggested by our results but lacking sufficient sampling to optimise
636 computationally. The apomorphic losses of Acanthocephala are also added. The
637 topology is derived from the strict consensus tree based on a matrix of 68 taxa and
638 247 characters; the non-gnathiferans were omitted for clarity but were included in the
639 analyses in which synapomorphies were optimised; the precise systematic position of
640 Gnathostomulida has not been recovered in the strict consensus tree, but it is widely
641 considered as the sister group of other gnathiferans. Yellow rectangles represent
642 characters associated with jaw apparatus, green rectangles represent characters
643 associated with gut (including mouth and anus), red rectangles represent characters
644 associated with body shape, and grey rectangles represent characters associated with
645 other body structures. Characters that can be observed in *J. daohugouensis* are in red
646 colour, otherwise in black. Cross indicates extinct taxa.


a
mo?
pb
ja
tc
au?
bu
b
c
d
e
pb
tc
bu


a
b
e
b
mo?
at?
c
d
C Si K
e
g
h
k
j
f
g
h
i
i
j
k
l
l


a
b
e
f
b
d
c
d
e
tr
au?
dw
f
pd
bu
tc


a
Micrognathozoa
Acanthocephala
Seisonidea
Bdelloidea
Monogononta
Eurotatoria
b
Micrognathozoa
Monogononta
Bdelloidea
Seisonidea
Acanthocephala
Hemirotifera
Pararotatoria
c
Micrognathozoa
Seisonidea
Monogononta
Bdelloidea
Acanthocephala
Lemniscea
d
Acanthocephala
†Juracanthocephalus
Loss of jaw apparatus
Seisonidea
Hooked proboscis
Bursa
Monogononta
Bdelloidea
Epidermis containing larger filament bundles
Pharyngeal region strongly depressed
Pararotatoria
Micrognathozoa
Anterior insertion of sperm flagellum
Syncytial epidermis with an intra-syncytial lamina
Multiciliated terminal cells of protonephridia
Loss of ventral locomotory cilia
Syndermata (Rotifera)
Gnathostomulida
Loss of unpaired basal plate
Trophi with unci
Dorsal anus
Gnathifera
Jaw apparatus
Alimentary tract
Body shape
Other body structures